Electronic Supporting Information for:

The Role of Metal-Organic Frameworks in Moderating Platinum-Based Ethanol Electrooxidation Catalysts

*Jana B. Fritzke, Claudia Eßbach, Philipp Wollmann, Arafat H. Khan, Irena Senkovska, Inez M. Weidinger, Stefan Kaskel, Eike Brunner**

Technische Universität Dresden, 01062 Dresden, Germany

1. CHARACTERIZATION OF THE CATALYST

1.1 PHYSICO-CHEMICAL CHARACTERIZATION

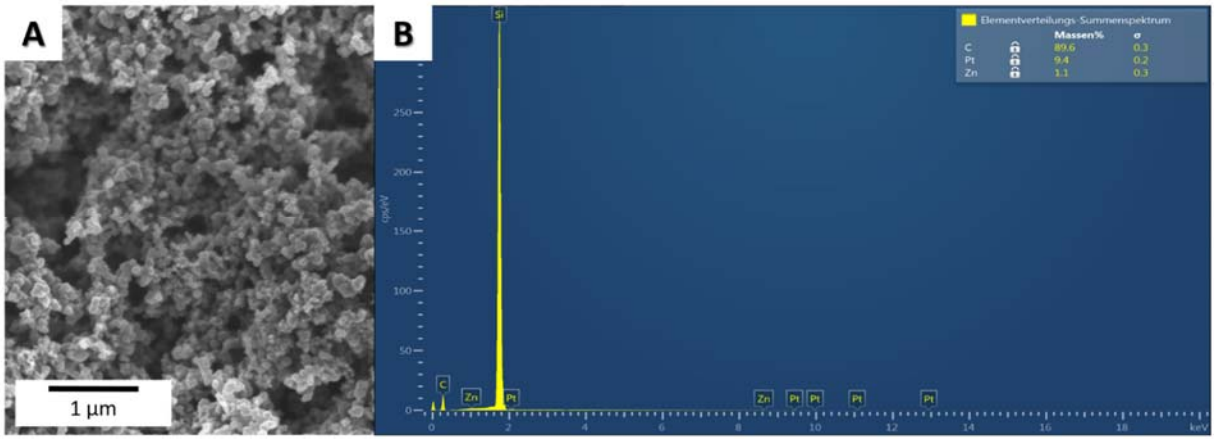

Figure S1. A: SEM image of the composite material Vulcan XC 72R / Pt with ZIF-8. **B:** EDX analysis of the functionalized catalyst.

The scanning electron microscopy (SEM) images show that the catalyst material exhibits aggregates formed from spherical particles (Figure S1 A), as is already known for the structure of carbon black.[1] The functionalisation with ZIF-8 has no significant visible influence on the morphology of the catalyst. In the EDX analysis (Figure S1 B), the main components of the catalyst are detectable: carbon, platinum and zinc.

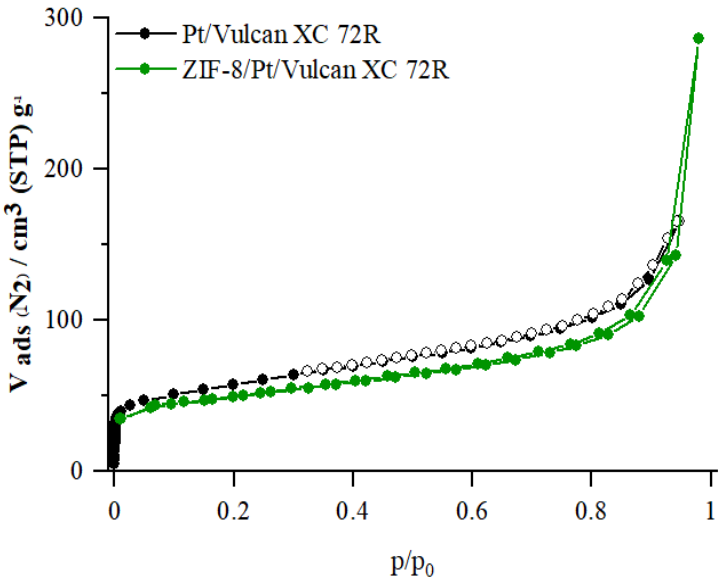

Figure S2. Comparison of the N_2 physisorption isotherms (77 K) of the unmodified catalyst Vulcan XC 72R / Pt (black) and the composite material Vulcan XC 72R / Pt / ZIF-8 (green).

The nitrogen physisorption isotherms measured at 77 K show slightly lower nitrogen uptake of the composite material compared to commercial catalyst (Figure S2). The catalyst Vulcan XC 72R/Pt consists mainly of micropores with 0.25 cm^3g^{-1} total pore volume (estimated at p/p_0 = 0.94). A pore volume of 0.22 cm^3g^{-1} could be determined for the composite material, which is in the same range of the unmodified catalyst. This fact could be explained by the low amount of the MOF, hence, ZIF-8 has a low contribution to the total pore volume. Only slight differences are detectable for the calculated BET surface. The composite material has a surface area of 179 m^2g^{-1} and the commercial catalyst 195 m^2g^{-1}. As already mentioned by Eßbach et al. the surface and the pore volume are influenced by the functionalization with ZIF-8, but this effect only occurs with larger loadings.[2]

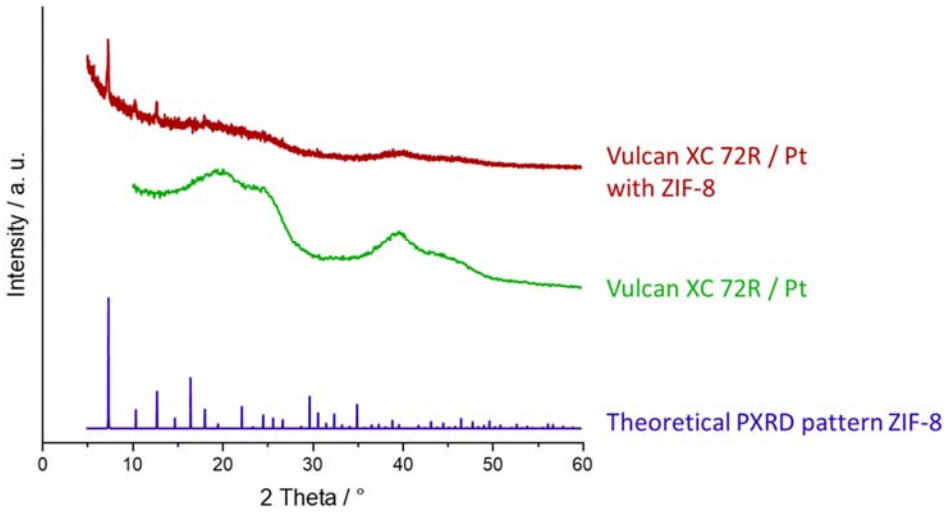

Figure S3. PXRD patterns of Vulcan XC 72R / Pt with ZIF-8 (red), Vulcan XC 72R / Pt (green) and theoretical PXRD pattern for ZIF-8 (violet).

The powder X-ray diffraction (PXRD) measurements show reflections in the 2θ range between 15° to 25°, which indicates that the catalyst Vulcan XC 72R (Figure S3 green) is an intermediate between graphitic and amorphous structure that is also called turbostratic. Additional reflexes at 2θ of 40° and 47° can be assigned to the fcc structure of Pt(111) and Pt(200), which result from the platinum nanoparticles of the catalyst.[3] In comparison, the diffractogram of the composite material (Figure S3 red) shows sharp reflections in the 2θ range of 5° to 20° in addition to the characteristic pattern of the commercial catalyst. This pattern matches with the calculated PXRD reflection pattern of ZIF-8 (Figure S3 violet) and indicates that ZIF-8 crystals are formed on the catalyst material.

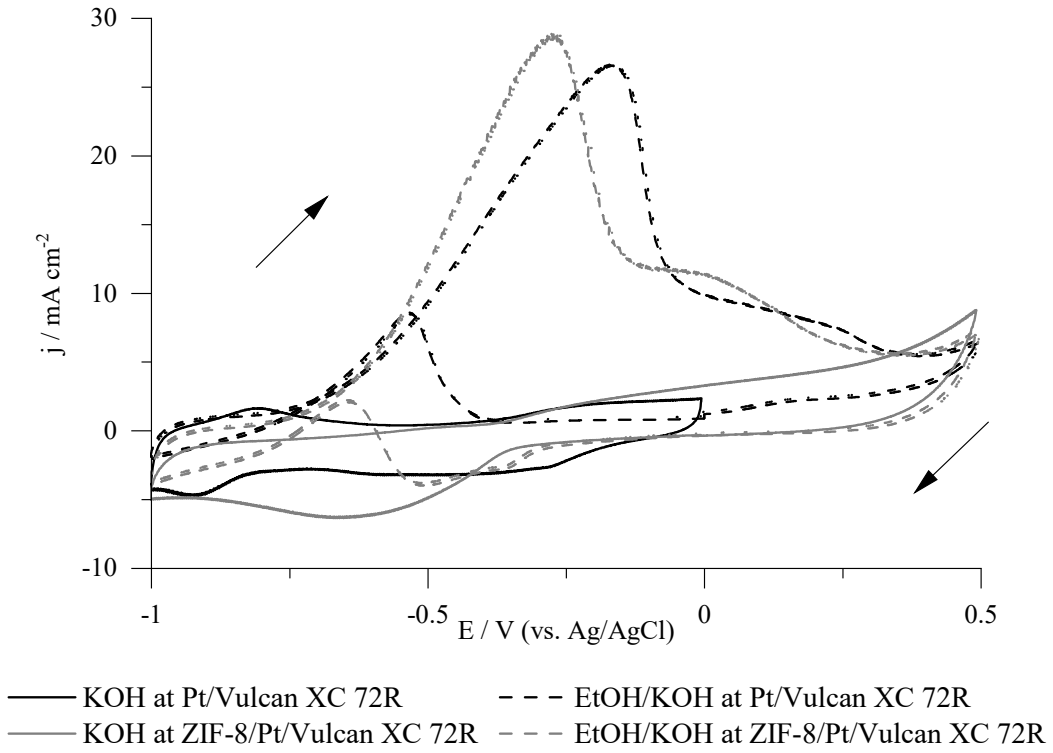

Figure S4. CV response of both studied materials in 0.5 M KOH and 0.5 M KOH with 0.5 M ethanol.

The CV response of Pt/C and of ZIF-8 functionalized Pt/C in pure electrolyte and ethanol containing electrolyte is investigated by rotating disk electrode (RDE) experiments. (Figure S4) The behaviour of Pt in alkaline media was already investigated and shows (i) the region of hydrogen underpotential deposition, (ii) the region of electrochemical double layer, (iii) the "butterfly" region of discharge of OH- to OH_{ads} and (iv) the region of oxidation of Pt to unknown oxides.[4,5] For the catalyst with ZIF-8, the accessibility by KOH is limited. Therefore, these signals are less intense. The ethanol oxidation reaction at Pt based catalysts is observed in the region between -0.5 to -0.1 V vs. Ag/AgCl. Hydrogen underpotential deposition is suppressed by adsorbed species from electrolyte solution. After oxidation of adsorbed species, oxidation of the

Pt surface is observed (0 – 0.2 V vs. Ag/AgCl). In the cathodic sweep, the Pt catalyst is reactivated by reduction of the oxides. With increasingly negative potential, further oxidation of ethanol and other adsorbed species takes place.[6] As a consequence of ZIF-8 functionalization of this Pt-containing catalyst, signals are shifting towards more negative potentials.[2]

1.2 ICP-OES

The samples are analysed with an Optima 7000DV spectrometer (Perkin Elmer) utilizing the following parameters: liquid flow 1.6 l min^{-1}, plasma gas flow 15 l min^{-1}, auxiliary gas flow 0.2 l min^{-1}, nebulizer gas flow 0.65 l min^{-1} and 2-point background correction. The chosen spectral lines detected in axial direction were 327.393 nm for Cu, 238.204 nm for Fe, 231.604 nm for Ni, and 340.458 nm for Pd. The detected concentrations of the elements are summarized in Table S 1.

Table S1. Results of the ICP-OES investigation of the commercial catalyst Vulcan XC 72R / Pt.

	Cu / mg g^{-1}	Fe / mg g^{-1}	Ni / mg g^{-1}	Pd / mg g^{-1}
Vulcan XC 72R / Pt	0.046	0.651	0.058	0.031

The elements Fe, Cu, Ni and Pd are detected in small amounts in the commercial catalyst. Pd has already been intensively studied as an alternative for platinum catalysts for the electro-oxidation of ethanol.[7] Ni and Fe as an alloy with Co were also examined as electrode material for the oxidation of alcohols.[8] Therefore, an influence of these elements on the investigated catalytic reaction cannot be excluded.

2. SOLID STATE NMR SPECTROSCOPY

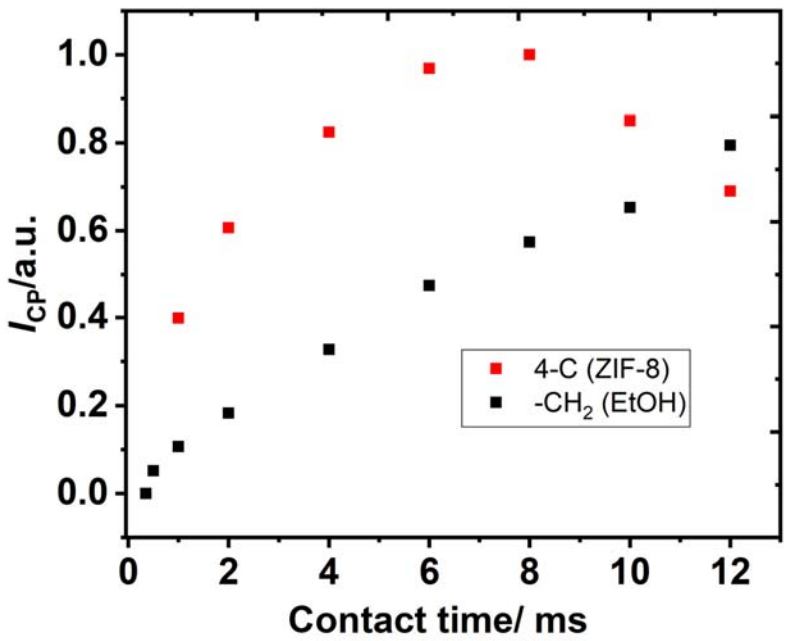

Figure S5. ^{13}C CP MAS NMR signal intensity of adsorbed ethanol measured as a function of contact time. For comparison, the intensity of the 4-C signal of ZIF-8 is also shown in red.

Figure S5 displays the mixing time dependence of the ^{13}C CP MAS NMR signal of a carbon atom located on ZIF-8 (4-C) and of the signal due to adsorbed ethanol inside the pores of the MOF at 57.8 ppm (see below). Note that the signal of adsorbed ethanol steadily builds up over the entire considered contact time range. In contrast, the 4-C signal of ZIF-8 starts decaying beyond ca. 8 ms contact time due to $T_{1\rho}$ relaxation.

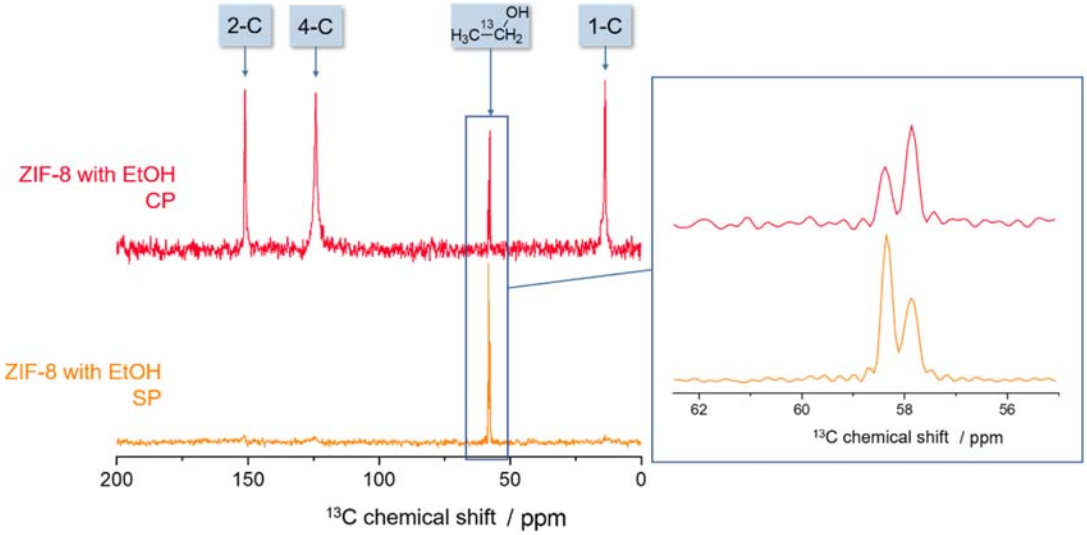

Figure S6. ^{13}C solid-state NMR spectra of ZIF-8 loaded with ethanol-containing electrolyte. Top: CP spectrum measured with 4 ms mixing time. Bottom: Directly excited (SP) spectrum.

A second ethanol signal can sometimes be observed depending on the loading and rotor packing in addition to the signal at 57.8 ppm (see Figure S6). If present, this second signal occurs at 58.4 pm. The ring current effect in carbon materials induces a diamagnetic shift of the signals of adsorbed molecules, i.e., to lower chemical shift values.[9] It is thus assumed that the latter signal is due to ethanol inside the pores of the MOF. The other, rotor-packing dependent signal may then be attributed to ethanol outside the MOF particles. This is corroborated by the CP spectrum. The CP efficiency at a contact time of 4 ms is higher for the signal of in-pore ethanol at 57.8 ppm. Since this value is in the contact time regime governed by the dipole coupling-dependent CP build-up time constant (cf. Figure S5), a stronger immobilization of this species can be concluded as expected for in-pore adsorbed ethanol at 57.8 ppm. In addition to ethanol, the expected signals of the ZIF-8 linker molecules (cf. Figure 3B) are visible in the CP spectrum. They are not detectable in the SP experiment due to the low natural abundance of ^{13}C in the linkers of ZIF-8.

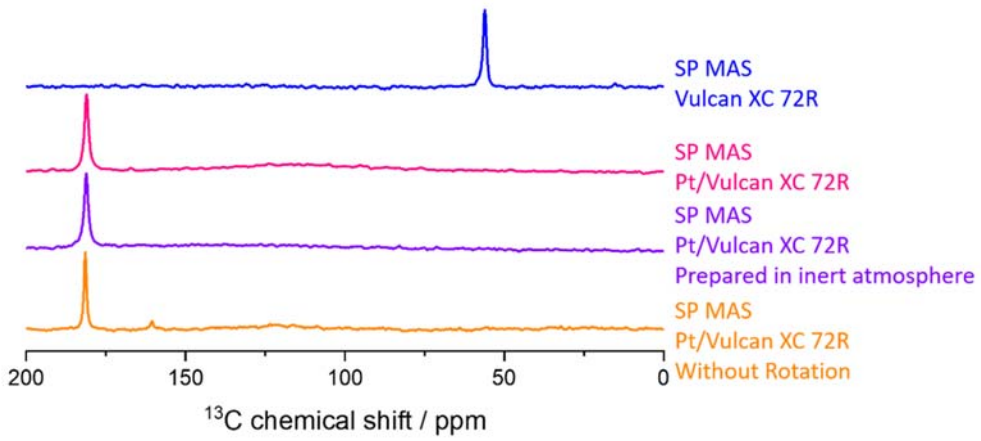

Figure S7. Solid-state NMR spectroscopy of the carbon Vulcan XC 72R and the catalyst Vulcan XC 72R / Pt soaked with the ^{13}C labeled electrolyte. An influence of the preparation under inert gas atmosphere and rotation on the oxidation reaction could not be detected.

Additional solid-state NMR spectroscopic investigations are carried out in order to determine the influence on the complete oxidation reaction in more detail. On the one hand, the sample was prepared under N_2 atmosphere. The incipient wetness method is carried out in an inert gas-flooded glove tent and the NMR rotor is filled under this atmosphere. It is visible in the spectra that the oxygen of the air had no influence on the complete oxidation of the ethanol to acetic acid in the rotor, since no ethanol is detectable (Figure S violet). On the other hand, a sample without rotation at the magic angle is measured. A widespread signal could be detected due to the anisotropic interactions. However, only the signal of the oxidation product acetic acid is detectable in this experiment (Figure S orange). Concluding, the effects of rotation, especially heating the sample, do not contribute to the oxidation of the electrolyte. Therefore, the influence of magnetically induced catalysis can no longer be excluded.

3. *IN SITU* RAMAN SPECTROSCOPY

The cyclic voltammetry measurements were carried out to characterize the used *in situ* cells. An overview of the electrochemical behavior of the cells can be obtained, but no further comparison of the detected voltages with data from literature can be made due to the lack of a reference electrode. It is clearly visible that the CVs of the *in situ* cells show an offset of approx. 0.7 V in comparison with the CV response referenced against Ag / AgCl (Figure S8) which corresponds to the difference between reference electrode and CE. The CV of the catalyst Vulcan XC 72R/Pt within the Raman spectro-electrochemical cell shows the typical features of the alcohol oxidation reaction. At 0.5 V, the ethanol oxidation takes place. In the reversed scan, the reduction of the oxidized Pt species can be observed at 0.6 V.[10] Oxidation of Pt is not detectable but should take place at higher voltages than the ethanol oxidation. The ethanol oxidation is an irreversible reaction, but in the reversed scan, an additional oxidation signal can be observed around -0.08 V. This signal can be assigned to the desorption of the products from the catalyst surface.[11]

Since the oxidation voltage of ethanol occurs at 0.5 V for this kind of electrochemical cell. Raman spectra are recorded up to a potential of 0.6 V.

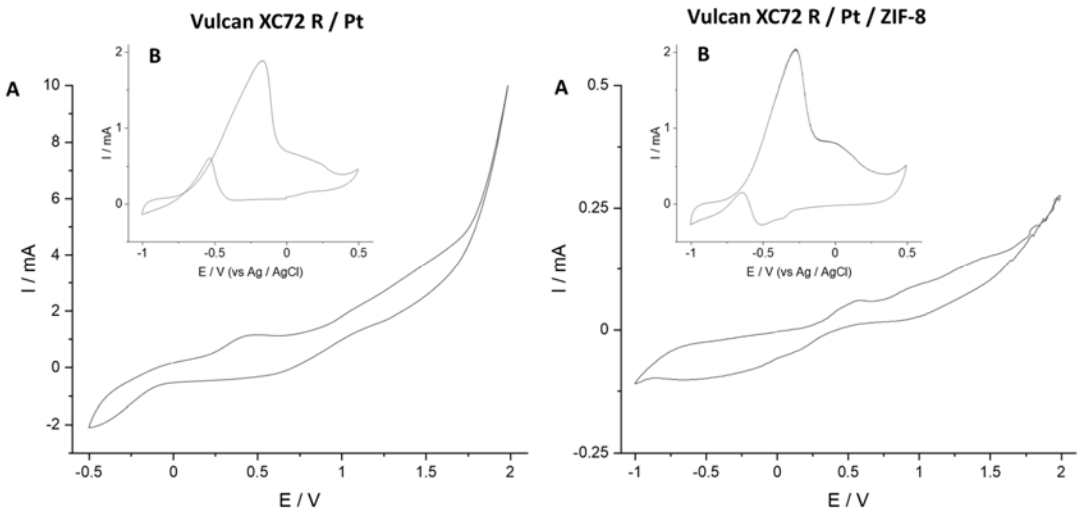

Figure S8. **A** Cyclic voltammetry curves of the *in situ* Raman cells with the unmodified catalyst and the ZIF-8-modified catalyst at the WE in aqueous solution of 0.5 M KOH with 0.5 M ethanol. Scan rate: 100 mV/s in comparison **B** cyclic voltammetry response of the catalysts investigated with RDE experiments.

The CV curve of a Raman cell with the functionalized catalyst at WE (Figure S) is similar to the one of pure catalyst but with shifted signals (ethanol oxidation at 0.6 V and Pt oxidation at 1.5 V in the anodic scan, reduction of oxidative species at Pt at -0.6 V and oxidation of desorbed species at 0.5 V in the cathodic scan).[10,11] Based on this, Raman measurements are carried out in 100 mV steps up to the voltage of 0.7 V.

Measurements of *in situ* Raman spectra on a cell with ethanol-free aqueous 0.5 M KOH electrolyte (CE: Vulcan XC 72R, WE: Vulcan XC 72R/Pt) reveal the absence of significant changes in the spectrum at increasing applied voltage (Figure S9). In the spectra, the typical vibration modes of the carbon electrodes are detectable. The D* band at 2686 cm^{-1}, the characteristic G (1598 cm^{-1}) and D1 bands (1354 cm^{-1}) of graphite, as well a shoulder of the G band at 1624 cm^{-1} is suggesting

the presence of carbonyl groups on the surface of the lattice.[10,11,12] Furthermore, the I band near 1200 cm^{-1} occurs which could be assigned to the vibration mode of sp^3 carbons and terminal C-O bonds.[13,14]

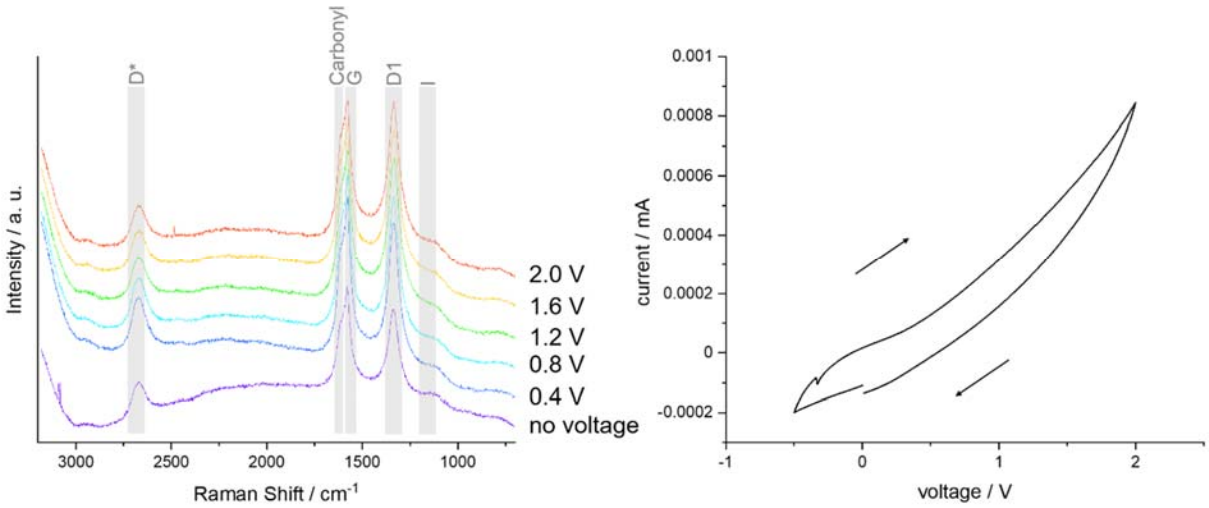

Figure S9. Spectra of the *in situ* cell with the commercial catalyst at WE, carbon black at CE and 0.5 M KOH electrolyte recorded at different voltages (left). The corresponding CV curve of the *in situ* Raman cell recorded with 100 mV/s scan rate (right).

In a cell without ethanol no characteristic electrochemical reactions such as transformation or degradation of the electrodes are observed in the CV response of the investigated Raman cell.

4. CHRONOAMPEROMETRIC MEASUREMENTS OF THE POUCH CELLS

Recorded chronoamperograms show constant voltage and decreasing current over the whole measurement time. The observed fluctuations in the current and voltage curves result from the desorption of the products from the catalyst surface.[12]

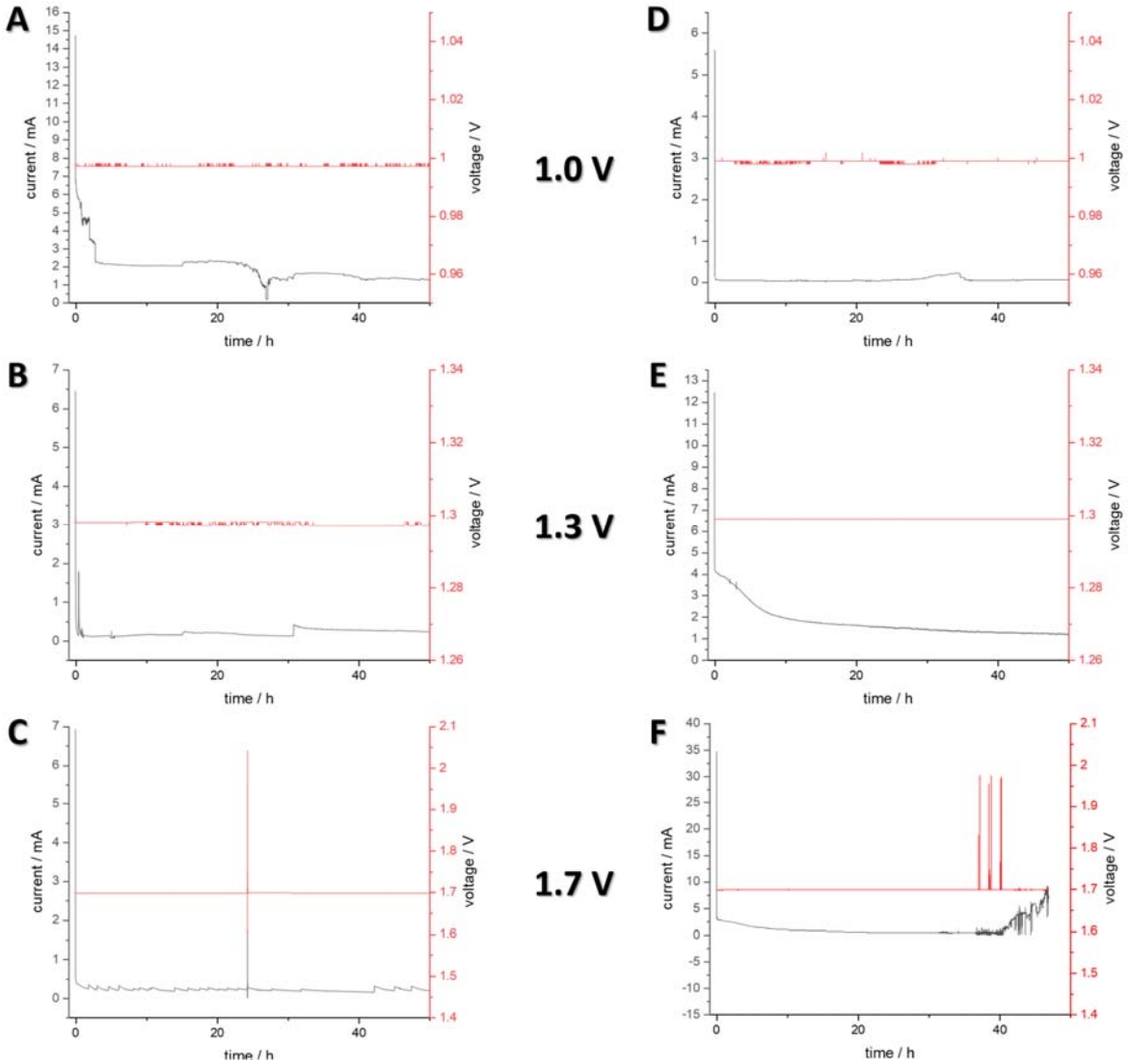

Figure S10. Chronoamperometric measurements within the *in situ* NMR spectroscopic investigations of pouch cells at different voltages. **A-C** measurements of pouch cells with the commercial catalyst Vulcan XC 72R / Pt at the WE and **D-F** measurements of pouch cells with the composite material at the WE.

AUTHOR INFORMATION

Corresponding Author

*E-mail: Eike.Brunner@tu-dresden.de

ABBREVIATIONS

BET, Brunauer–Emmett–Teller; CE, counter electrode; EDX, energy-dispersive x-ray analysis; ICP-OES, inductive coupled plasma optical emission spectrometry; MOF, Metal-organic framework; PXRD, powder x-ray diffraction; RDE: rotating disk electrode; SEM, scanning electron microscopy; ZIF, zeolitic imidazolate framework

REFERENCES

(1) Hess, William M.; Herd, C. R. Carbon Black: Science and Technology; Donnet, Jean-Baptiste; Bansal, Roop Chand; Wang, M.-J., Ed.; CRC Press, Taylor & Francis Group: Boca Raton; London; New York, 1993; p 89.

(2) Eßbach, C.; Senkovska, I.; Unmüssig, T.; Fischer, A.; Kaskel, S. Selective Alcohol Electrooxidation by ZIF-8 Functionalized Pt/Carbon Catalyst. *ACS Appl. Mater. Interfaces* **2019**, *11* (23), 20915–20922.

(3) Lázaro, M. J.; Calvillo, L.; Celorrio, V.; Pardo, J. I.; Perathoner, S.; Moliner, R. *Carbon Black: Production, Properties and Uses-STUDY AND APPLICATION OF CARBON BLACK VULCAN XC-72R IN POLYMERIC ELECTROLYTE FUEL CELLS M.J.*; Sanders, I. J., Peeten, T. L., Eds.; Nova Science Publishers, Inc., 2011.

(4) Schmidt, T. J.; Stamenkovic, V.; Arenz, M.; Markovic, N. M.; Ross, P. N. Oxygen Electrocatalysis in Alkaline Electrolyte: Pt(Hkl), Au(Hkl) and the Effect of Pd-Modification. *Electrochim. Acta* **2002**, *47* (22–23), 3765–3776.

(5) Schmidt, T. J.; Ross, P. N.; Markovic, N. M. Temperature-Dependent Surface Electrochemistry on Pt Single Crystals in Alkaline Electrolyte: Part 1: CO Oxidation. *J. Phys. Chem. B* **2001**, *105* (48), 12082–12086.

(6) Lai, S. C. S.; Koper, M. T. M. Ethanol Electro-Oxidation on Platinum in Alkaline Media. *Phys. Chem. Chem. Phys.* **2009**, *11* (44), 10446–10456.

(7) Sheikh, A. M.; Silva, E. L.; Moares, L.; Antonini, L. M.; Abellah, M. Y.; Malfatti, C. F. Pd-Based Catalysts for Ethanol Oxidation in Alkaline Electrolyte. *Am. J. Min. Metall.* **2014**, *2* (4), 64–69.

(8) Spendelow, J. S.; Wieckowski, A. Electrocatalysis of Oxygen Reduction and Small Alcohol Oxidation in Alkaline Media. *Phys. Chem. Chem. Phys.* **2007**, *9* (21), 2654–2675.

(9) Forse, A. C.; Griffin, J. M.; Presser, V.; Gogotsi, Y.; Grey, C. P. Ring Current Effects: Factors Affecting the NMR Chemical Shift of Molecules Adsorbed on Porous Carbons. *J. Phys. Chem. C* **2014**, *118* (14), 7508–7514.

(10) Tripković, A. V.; Popović, K. D.; Momčilović, J. D.; Draić, D. M. Kinetic and Mechanistic Study of Methanol Oxidation on a Pt(111) Surface in Alkaline Media. *J. Electroanal. Chem.* **1996**, *418* (1–2), 9–20.

(11) Tripković, A. V.; Popović, K. D.; Lović, J. D. The Influence of the Oxygen-Containing Species on the Electrooxidation of the C1–C4 Alcohols at Some Platinum Single Crystal Surfaces in Alkaline Solution. *Electrochim. Acta* **2001**, *46* (20–21), 3163–3173.

(12) Huang, L.; Sorte, E. G.; Sun, S. G.; Tong, Y. Y. J. A Straightforward Implementation of in Situ Solution Electrochemical ^{13}C NMR Spectroscopy for Studying Reactions on Commercial Electrocatalysts: Ethanol Oxidation. *Chem. Commun.* **2015**, *51* (38), 8086–8088.